

# N-Arachidonoyl-Dopamine Tunes Synaptic Transmission onto Dopaminergic Neurons by Activating both Cannabinoid and Vanilloid Receptors

Silvia Marinelli<sup>\*1</sup>, Vincenzo Di Marzo<sup>2</sup>, Fulvio Florenzano<sup>3</sup>, Filomena Fezza<sup>4</sup>, Maria Teresa Viscomi<sup>3</sup>, Mario van der Stelt<sup>2</sup>, Giorgio Bernardi<sup>1,5</sup>, Marco Molinari<sup>3</sup>, Mauro Maccarrone<sup>4,6,7</sup> and Nicola B Mercuri<sup>1,5,7</sup>

<sup>1</sup>Experimental Neurology, IRCCS Fondazione Santa Lucia, Rome, Italy; <sup>2</sup>Endocannabinoid Research Group, Istituto di Chimica Biomolecolare, Consiglio Nazionale delle Ricerche, Pozzuoli, Naples, Italy; <sup>3</sup>Experimental Neurorehabilitation Labs, IRCCS Santa Lucia Foundation, Rome, Italy; <sup>4</sup>Department of Biomedical Sciences, University of Teramo, Teramo, Italy; <sup>5</sup>Dipartimento di Neuroscienze, Università di Tor Vergata, Rome, Italy; <sup>6</sup>IRCCS C. Mondino, Mondino-Tor Vergata Center for Experimental Neurobiology, Rome, Italy

In the present study, we used electrophysiological, biochemical, and confocal microscopy techniques, to investigate the functional role of transient receptor potential vanilloid type 1 (TRPV1) and cannabinoid type 1 receptors (CB1-R) in the substantia nigra pars compacta (SNpc) and their stimulation by the endocannabinoid N-arachidonoyl-dopamine (NADA). Liquid chromatography–mass spectrometry analyses revealed that a NADA-like compound is produced in substantia nigra slices, in conditions of hyperactivity. Moreover, the functional role of both TRPV1 and CB1-R in modulating synaptic transmission in this area was suggested by confocal microscopy data, showing TRPV1 and CB1-R immunoreactivity in punctate structures, probably representing synaptic contacts on cell bodies of the SNpc. In patch-clamp recordings from dopamine (DA) neurons of the SNpc, we found that NADA increases or reduces glutamatergic transmission onto DA neurons by activating TRPV1 and CB1 receptors, respectively, whereas it decreases GABAergic transmission via CB1 stimulation. Facilitation of glutamate release through TRPV1 was blocked in the presence of a selective blocker of the putative endocannabinoid membrane transporter (EMT), indicating that NADA needs to be taken up by cells to interact with this receptor. In line with these data, biochemical results demonstrated that NADA selectively acted at CB1-R when its re-uptake was blocked. Altogether these data demonstrate a significant role exerted by the endocannabinoid/endovanilloid NADA in the regulation of synaptic transmission to DA neurons of the SNpc. Moreover, they highlight a key function of the EMT transporter in promoting the stimulation of TRPV1 or CB1-R, thus favoring facilitation or inhibition of glutamate synaptic release.

*Neuropsychopharmacology* (2007) **32**, 298–308. doi:10.1038/sj.npp.1301118; published online 7 June 2006

**Keywords:** NADA; TRPV1; cannabinoid receptors; patch-clamp recordings; confocal microscopy; endocannabinoid transporter

## INTRODUCTION

N-arachidonoyl-dopamine (NADA) and anandamide (AEA) (Al-Hayani *et al*, 2001; Di Marzo *et al*, 2001; Huang *et al*, 2002b; Marinelli *et al*, 2003; Sagar *et al*, 2004) are endogenous lipids of the central nervous system (CNS), acting on both ionotropic transient receptor potential vanilloid type 1 (TRPV1; for a review see Caterina and Julius, 2001) and metabotropic cannabinoid type 1 receptors (CB1-R; reviewed by Howlett, 2002). We have previously shown a

functional role of TRPV1 in the ventral midbrain (Marinelli *et al*, 2003, 2005) and other studies have demonstrated a presynaptic modulation of neurotransmission by CB1 in the same area (Szabo *et al*, 2002a; Melis *et al*, 2004). Compared with AEA, NADA is more potent at TRPV1 and less potent but more efficacious at CB1-R (Bisogno *et al*, 2000; Bezuglov *et al*, 2001; Huang *et al*, 2002b).

In dorsal root ganglia (DRG) neurons, NADA depolarizes the membrane potential and increases intracellular calcium through TRPV1 and CB1-R stimulation, whereas it increases substance P and calcitonin gene-related peptide (CGRP) release via TRPV1 in slices of rat dorsal spinal cord (Huang *et al*, 2002b; Sagar *et al*, 2004). In the hippocampus, NADA enhances paired-pulse depression through an increase of GABAergic transmission (Huang *et al*, 2002b). Besides these *in vitro* effects, NADA induces thermal hyperalgesia, stimulates spontaneous and heat-evoked activity in spinal nociceptive neurons (Huang and Walker, 2006), and exerts

\*Correspondence: Current address: Dr S Marinelli, European Brain Research Institute (EBRI), Via del Fosso di Fiorano, 64 Rome, Italy; Tel: +39 06501703127, Fax: +39 06501703315, E-mail: s.marinelli@ebri.it  
<sup>7</sup>Equally senior authors.

Received 14 November 2005; revised 27 April 2006; accepted 28 April 2006

Online publication: 11 May 2006 at <http://www.acnp.org/citations/Npp051106050678/default.pdf>

a contractile action on smooth muscles by acting on TRPV1 (Huang *et al*, 2002b; Harrison *et al*, 2003; Price *et al*, 2004), while it causes analgesia, hypothermia, and catalepsy by activation of CB1-R (Bisogno *et al*, 2000). Finally, NADA exerts vasorelaxant effects by acting on both CB1-R and TRPV1 in small mesenteric vessels (O'Sullivan *et al*, 2004). Together, these studies indicate that NADA can behave as either an endovanilloid or endocannabinoid, depending on whether it interacts with TRPV1 or CB1-R, respectively.

Anatomical studies have found an immunocytochemical distribution of CB1-R (Julian *et al*, 2003; Tsou *et al*, 1998; Pettit *et al*, 1998) and TRPV1 (Mezey *et al*, 2000; Szabo *et al*, 2002b; Toth *et al*, 2005) in the same brain nuclei. The expression of both receptors was not confined only to neurons, but has been reported also in astrocytes for TRPV1 and in glial cells for CB1-R (Doyle *et al*, 2002; Toth *et al*, 2005; Pazos *et al*, 2005). In addition, there is evidence of a high degree of colocalization of CB1-R and TRPV1 in DRG neurons, enriched mesencephalic cultures, hippocampus, and cerebellum (Ahluwalia *et al*, 2000, 2002; Kim *et al*, 2005; Cristino *et al*, 2006). However, there have been no reports on the colocalization of both receptors at synaptic level.

Thus, the aim of the present study is to analyze the anatomical distribution of TRPV1 and CB1-R in slices of substantia nigra by confocal microscopy and the effects of NADA onto these receptors, by electrophysiological recordings.

Being an endogenous chemical signal, NADA signaling can be regulated by acting on both its membrane transport system and metabolism (Di Marzo *et al*, 1994; Beltramo *et al*, 1997; Cravatt *et al*, 2001; Fegley *et al*, 2004). In particular, NADA is rapidly taken up by C6 glioma cells via the putative endocannabinoid transporter (EMT), although it is only slowly hydrolyzed by fatty acid amide hydrolase to dopamine (DA) and arachidonic acid (Huang *et al*, 2002b).

Therefore, in this study, we also attempted to separate vanilloid and cannabinoid effects evoked by NADA by blocking the activity of EMT in slices of substantia nigra pars compacta (SNpc) using electrophysiological and biochemical techniques.

## METHODS

### Slice Preparation and Patch-Clamp Technique

Wistar rats (12–24 days old) were anesthetized with halothane and killed by decapitation. All experiments followed international guidelines on the ethical use of animals from the European Communities Council Directive of 24 November 1986 (86/609/EEC). The brain was rapidly removed from the skull and horizontal midbrain slices (300  $\mu$ m) were cut in cold artificial cerebrospinal fluid (ACSF) using a vibratome and left to recover at 33°C for at least 1 h. Slices were placed in a recording chamber and submerged in a continuously flowing (3 ml/min, 34°C) ACSF. ACSF composition was (in mM): NaCl 126; KCl 2.5; MgCl<sub>2</sub> 1.2; CaCl<sub>2</sub> 2.4; NaH<sub>2</sub>PO<sub>4</sub> 1.2; NaHCO<sub>3</sub> 19; glucose 10.

Neurons were visualized using infrared Nomarski optics on an upright microscope (Olympus BX50WI). Patch-clamp recordings were obtained using glass electrodes (3–4 M $\Omega$ ) filled with (in mM): K-methylsulfate 150; MgCl<sub>2</sub> 2; EGTA 0.1; HEPES 10; MgATP 2 mM; Na<sub>3</sub>GTP 0.3 for spontaneous excitatory postsynaptic current (sEPSC), whereas for the

recordings of spontaneous GABAergic postsynaptic current (sIPSC) K-methylsulphate was substituted with KCl 140.

Whole-cell patch-clamp (–60 mV holding potential) recordings were obtained using an Axopatch 1D (Axon Instruments) from 54 DA neurons of the SNpc. All recorded neurons were located rostrally, with respect to the medial terminal nucleus of the accessory optic tract. DA neurons were identified both visually and on the basis of their electrophysiological properties, by the presence of a prominent time-dependent  $I_h$ , in response to hyperpolarizing voltage steps (Mercuri *et al*, 1996). sEPSCs and sIPSCs were filtered at 1 kHz, digitized at 10 kHz, and recorded on computer using the pClamp9 software (Axon Instruments). Series resistance (8–15 M $\Omega$ ) was not compensated, in order to maintain the highest possible signal-to-noise ratio and neurons in which series resistance varied after drugs application by more than 10%, were rejected.

Glutamatergic and GABAergic synaptic events were isolated by recording in the presence of the GABA<sub>A</sub> receptor antagonist picrotoxin (100  $\mu$ M) and the ionotropic glutamate receptor antagonists CNQX (10  $\mu$ M) and AP5 (50  $\mu$ M).

### Statistical Analyses

Spontaneous events were detected and analyzed with Clampfit9 software (Axon Instruments), using a specific template waveform and an appropriate threshold (3.5–5) for each experiment. Each event was also visually inspected to prevent noise disturbance of the analysis.

In the figures, the cumulative interevent plots, obtained for each cell in control and after a specific treatment, were compared using the Kolmogorov–Smirnov (KS) test. The numerical data in the text are given as percentage  $\pm$  SEM of control (set to 100%) or as mean  $\pm$  SEM and compared using the Student's *t*-test or the  $\chi^2$  test.

Each slice received only a single exposure to NADA.

### Drugs

For the electrophysiological experiments, drugs were bath applied at the following final concentrations: picrotoxin (100  $\mu$ M), CNQX (10  $\mu$ M), AP5 (50  $\mu$ M), NADA (10  $\mu$ M), AM281 (500 nM), iodoresiniferatoxin (IRTX, 300 nM), (9Z)-N-(1-(R-4-Hydroxybenzyl)-2-hydroxyethyl)-9-octadecenamamide (OMDM-1, 1  $\mu$ M). NADA and OMDM-1 were synthesized at the Endocannabinoid Research Group (Pozzuoli, Italy). CNQX, AP5, AM281, WIN55,212-2 (WIN), and IRTX were purchased from Tocris Cookson (Bristol, UK).

NADA, AM281, and OMDM-1 were dissolved in ethanol. IRTX and WIN were dissolved in dimethyl sulfoxide (DMSO). The final concentration of DMSO and EtOH was less than 0.05%.

### Immunohistochemistry

Three adult male Wistar rats (body weight 200–250 g; Harlan, San Pietro al Natisone, UD, Italy) were perfused transcardially with 250 ml of saline followed by 250 ml of 4% paraformaldehyde in phosphate buffer (PB 0.1 M; pH 7.4), under general anesthesia induced by intraperitoneal injections of sodium pentobarbital (60 mg/kg). Each brain was removed from the skull, postfixed in the same fixative for

2 h and then transferred to 30% sucrose in PB at 4°C until it sank. Transverse sections, 40 µm thick, were cut at the level of the substantia nigra using a freezing microtome. Double immunofluorescence was carried out on free-floating sections incubated overnight in a mixture of the following antibodies: rabbit anti-TRPV1 N-terminus (1:100; Immunological Sciences) and mouse anti-tyrosine hydroxylase (TH; 1:500; Sigma) a marker for dopaminergic neurons; rabbit anti-TRPV1 and mouse antiglial fibrillary protein (GFAP; 1:400; Sigma), a marker for astrocytes; rabbit anti-TRPV1 and goat anti-CB1 N-terminus (1:100; Santa Cruz). All antibody solutions were prepared in PB and 0.3% Triton X-100 and each incubation step was followed by three washes in PB. After incubation with the cocktail of primary antibodies, the sections were incubated for 2 h at room temperature in a mixture of secondary immunoglobulin G antibodies including Cy3-conjugated donkey antirabbit and Cy2-conjugated donkey antimouse, or Cy2-conjugated donkey antigoat (1:100; Jackson ImmunoResearch Laboratories, West Grove, PA). Sections were then mounted on gelatin-coated slides, air dried, and cover slipped with GEL/MOUNT (Biomedica; Foster City, CA). Images were acquired through a confocal laser scanning microscope (Zeiss, LSM 510) equipped with an argon laser emitting at 488 nm and a helium/neon laser emitting at 543 nm. Plates were generated adjusting the contrast and brightness of digital images (Corel Draw, 9).

### Analysis of NADA in Midbrain Slices

Slices identical to those used for patch-clamp experiments were obtained by dissection and treated with either vehicle or 15 mM KCl for 15–18 min. After the stimulation, each slice was frozen in liquid nitrogen and stored at –80°C until lipid extraction. The latter was carried out with 5 v of a mixture of Tris-HCl 50 mM, pH 7.0, methanol, and chloroform (1:1:2, by volume) containing 50 pmol of d<sub>8</sub>-NADA. After homogenization, the aqueous phase was extracted two more times with an equal volume of chloroform, and the three organic phases were pooled and dried under a gentle flow of argon. The extract from each slice was directly analyzed by liquid chromatography coupled to electrospray ionization mass spectrometric analysis (LC-ESI-MS). As NADA is extremely unstable and easily oxidized, the analysis had to be carried out the same day of the extraction. LC-ESI-MS was carried out using a Shimadzu high-performance liquid chromatography (HPLC) apparatus (LC-10ADVP) fitted with a Phenomenex reverse phase column (5 µm, 150 × 4.5 mm<sup>2</sup>), eluted as described previously (Marsicano *et al*, 2002). The HPLC was coupled to a Shimadzu (LCMS-2010) quadruple MS via a Shimadzu ESI interface, the ESI source operating at 250°C and 1.7 keV and the quadruple monitoring positive ions. The analysis was carried out using the select ion monitoring (SIM) mode to improve sensitivity. Quantification was carried out by isotope dilution, that is, by comparing the areas of the peaks corresponding to native NADA with those of a known amount (10 pmol) of deuterated-NADA (NADA with 8-deuterium instead of hydrogen atoms on the fatty acyl moiety, d<sub>8</sub>-NADA) as an internal standard. Selected ions were set at *m/z* = 440 (quasimolecular ion, M + 1) and 441 (M + 2) for NADA and at *m/z* = 448 (quasimolecular ion, M + 1) and 449 (M + 2) for d<sub>8</sub>-NADA, and the amount of

endogenous NADA in stimulated tissue were quantified by calculating the ratio of the areas of the peaks eluting after 17.3 min and corresponding to native and d<sub>8</sub>-NADA, with a sensitivity threshold of 0.5 ± 0.1 pmol, and a reproducibility of 89.5 ± 3.5% (means ± SE, *n* = 10). The peak area ratios between the quasi molecular ions of d<sub>8</sub>-NADA (10 pmol) and d<sub>0</sub> NADA varied in a linear way with respect to the peak areas of the quasimolecular ion of d<sub>0</sub> NADA in the 0.5–500 pmol range of concentrations of the latter.

### [<sup>3</sup>H]NADA Cellular Uptake

The [<sup>3</sup>H]NADA was synthesized by reacting [<sup>3</sup>H]-DA (20.50 Ci/mmol, from Perkin-Elmer Life Sciences, Boston, MA), diluted with unlabeled DA and an excess of arachidonoyl chloride in anhydrous dichloromethane (Huang *et al*, 2002b). The mixture was left at 4°C for 15 min, then the reaction mixture was purified by thin layer chromatography (TLC) developed in hexane:ethyl acetate:acetic acid (50/50/1, by volume). The final specific activity of [<sup>3</sup>H]NADA was 1 µCi/µmol.

The uptake of [<sup>3</sup>H]NADA by SN slices was performed as described recently for the uptake of [<sup>3</sup>H]AEA (Maccarrone *et al*, 2003; Fezza *et al*, 2006). Slices (three for each assay) were incubated for 15 min with 25 µM [<sup>3</sup>H]NADA, then they were washed three times in 2 ml phosphate-buffered saline (PBS) containing 1% bovine serum albumin and were finally resuspended in 200 µl PBS. Membrane lipids were then extracted, resuspended in 0.5 ml methanol, mixed with 3.5 ml Sigma-Fluor liquid scintillation cocktail for nonaqueous samples (Sigma), and radioactivity was measured in a LKB1214 Rackbeta scintillation counter (Amersham Pharmacia Biotech, Uppsala, Sweden). To discriminate non-carrier-mediated from carrier-mediated transport through cell membranes, [<sup>3</sup>H]NADA uptake at 37°C was compared with that at 4°C (Maccarrone *et al*, 2003).

Biochemical data reported in this paper are the mean (± SD) of three independent determinations, each in duplicate. Statistical analysis was performed by the nonparametric Mann-Whitney *U*-test, elaborating experimental data by means of the InStat 4 program (GraphPAD Software for Science).

## RESULTS

### A NADA-Like Lipid is Produced Upon High K<sup>+</sup> Stimulation of Rat Midbrain Slices

When analyzed by means of ESI-LC-MS, lipid extracts from rat midbrain slices did not exhibit any detectable amount of NADA. However, when the slices had been stimulated with 15 mM KCl, a small peak with the same retention time and molecular weight as NADA was detected. When quantified by isotope dilution with synthetic d<sub>8</sub>-NADA, this compound amounted to 3.3 ± 0.4 pmol/g wet weight tissue (mean ± SD, *n* = 5).

### NADA Increases or Decreases Glutamatergic Synaptic Transmission Via TRPV1 or CB1-R, Respectively

As TRPV1 and CB1-R modulate the excitability of DA neurons and NADA activates both receptors (Bisogno *et al*,

2000; Mezey *et al*, 2000; Moldrich and Wenger, 2000; Huang *et al*, 2002b; Szabo *et al*, 2002b; Julian *et al*, 2003; Marinelli *et al*, 2003, 2005; Melis *et al*, 2004), we performed experiments to assess the effect of NADA on glutamatergic synaptic transmission.

In the presence of the GABA<sub>A</sub> antagonist picrotoxin (100  $\mu$ M), the sEPSCs were blocked by the non-NMDA receptor antagonist, CNQX (10  $\mu$ M,  $n=5$ , Figure 1a). Superfusion of NADA (1  $\mu$ M) increased sEPSCs frequency by  $16.20 \pm 8.19\%$  of control ( $n=5$ ,  $p<0.05$ , Figure 1e), whereas it did not significantly affect the amplitude ( $8.02 \pm 1.12\%$ ;  $n=5$ ,  $p=0.47$ ). At higher concentrations, NADA showed neither a CB1- nor a TRPV1-mediated effect.

In fact, NADA (10  $\mu$ M) did not affect the frequency and the amplitude of sEPSCs (in control,  $6.61 \pm 1.33$  Hz and  $13.88 \pm 0.92$  pA, during NADA,  $5.94 \pm 1.93$  Hz and  $15.37 \pm 1.39$  pA,  $n=7$ ). However, when NADA (10  $\mu$ M) was applied together with the CB1 antagonist AM281 (500 nM), it significantly increased the frequency of sEPSCs by  $61.91 \pm 12.91\%$  of control (in control  $3.55 \pm 0.85$  Hz and with NADA  $5.84 \pm 0.8$  Hz;  $n=5$ ,  $p<0.05$ , Figure 1b and e) without affecting their amplitude ( $13.82 \pm 9.10\%$ ,  $12.78 \pm 6.39$  and  $13.59 \pm 7.26$  pA, in control and NADA, respectively,  $n=5$ ,  $p=0.22$ ). Similarly, NADA (3  $\mu$ M) together with AM281 (500 nM) enhanced the rate of sEPSCs by  $27.16 \pm 8.92\%$  ( $n=5$ ,  $p<0.05$ ; Figure 1d), whereas it did

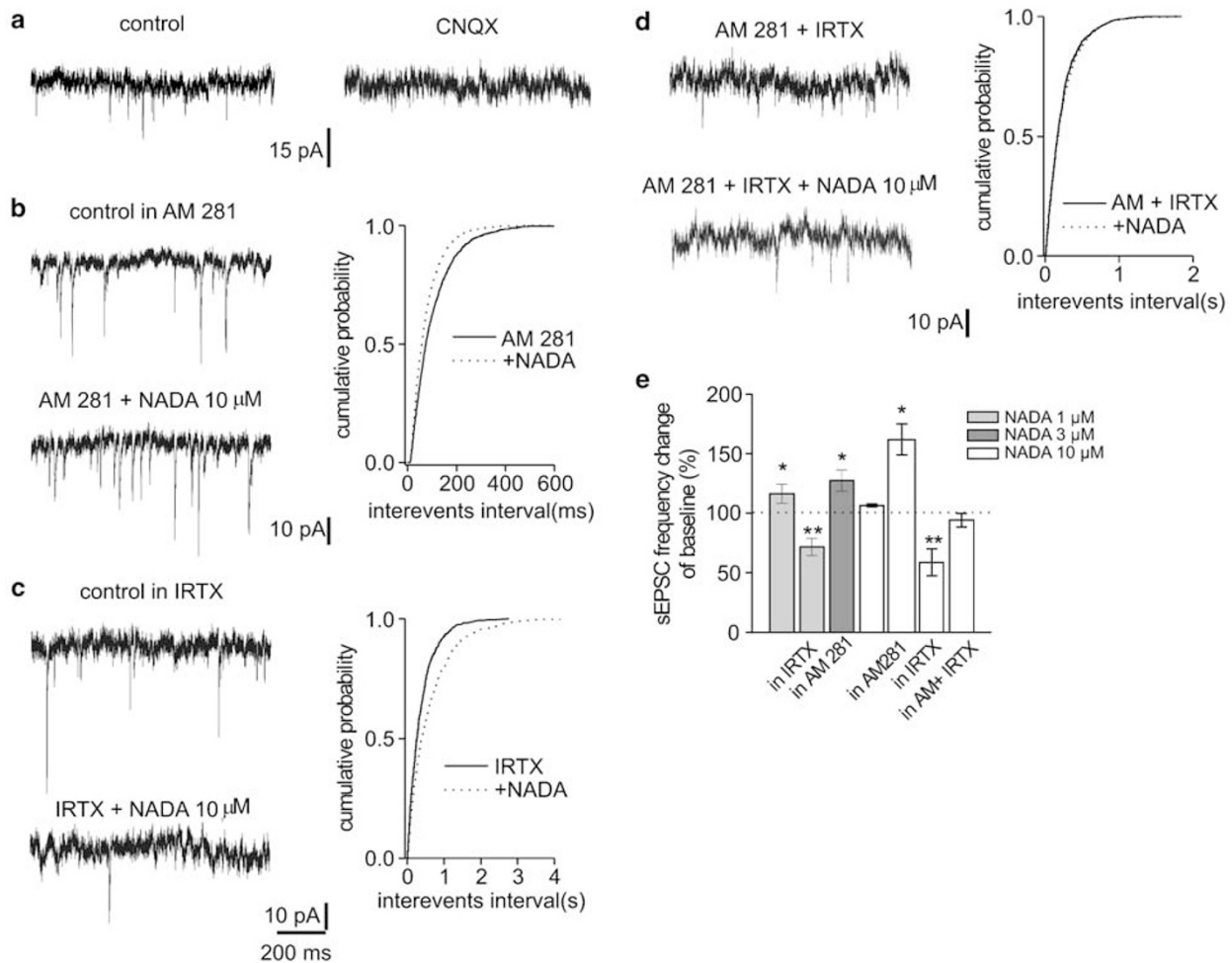


**Figure 1** Effects of NADA on sEPSCs of SNpc DA neurons. Recordings were performed in the presence of picrotoxin (100  $\mu$ M). (a) Bath perfusion of the selective AMPA receptor antagonist, CNQX (10  $\mu$ M), completely abolished sEPSCs (right panel). (b) In the presence of AM281 (500 nM), bath perfusion of NADA (10  $\mu$ M) for 3–5 min increased the frequency of sEPSCs. The top and bottom panels show trace records obtained before and during NADA, respectively. On the right, the cumulative probability distributions of interevent intervals from the neuron recorded on the left, in control (AM281, solid line), and during NADA (NADA + AM281, dotted line) are significantly different ( $p<0.02$ , KS test). (c) In the presence of IRTX (300 nM), bath perfusion of NADA (10  $\mu$ M) reduced the frequency of sEPSCs. The top and bottom panels show trace records obtained before and during NADA, respectively. On the right, the cumulative probability distributions of interevent intervals from the neuron recorded on the left, in control (IRTX, solid line), and during NADA (NADA + IRTX, dotted line) are significantly different ( $p<0.02$ , KS test). (d) In the presence of both IRTX and AM281, NADA did not modify the frequency of sEPSCs. The top and bottom panels show trace records, before and during NADA perfusion. On the right, the cumulative probability distributions of interevent intervals of the neuron recorded on the left, in the presence of IRTX and AM281 (solid line), and during NADA (+ AM281 and IRTX, dotted line) did not vary significantly ( $p=0.22$ , KS test). (e) Summary histogram of the effect of NADA (1  $\mu$ M) (% of control  $\pm$  SEM,  $n=5$ ), in the presence of the TRPV1 antagonist IRTX (% of control  $\pm$  SEM,  $n=12$ ); NADA (3  $\mu$ M) (% of control  $\pm$  SEM,  $n=5$ ); NADA (10  $\mu$ M) (% of control  $\pm$  SEM,  $n=7$ ), in the presence of the CB1-R antagonist, AM281 (% of control  $\pm$  SEM,  $n=5$ ), the IRTX 300 nM (% of control  $\pm$  SEM,  $n=6$ ), and of both IRTX and AM281 (% of control  $\pm$  SEM,  $n=6$ ). (\*\* $p<0.02$ , \* $p<0.05$ , Student's *t*-test paired).

not significantly affect their amplitude ( $11.65 \pm 0.97\%$ ,  $p = 0.085$ ).

To test whether low doses of NADA are able to activate CB1-R as well, NADA ( $1 \mu\text{M}$ ) was added to the bath perfusion in the presence of the TRPV1 antagonist, IRTX. Superfusion of IRTX ( $300 \text{ nM}$ ) decreased *per se* the frequency of sEPSCs compared to the control (from  $10.64 \pm 3.4$  to  $8.65 \pm 2.75 \text{ Hz}$ ,  $n = 12$ ,  $p < 0.05$ ) without affecting their amplitude ( $11.54 \pm 0.57$ – $10.50 \pm 0.52 \text{ pA}$ ,  $n = 12$ ,  $p = 0.09$ ). Simultaneous application of NADA ( $1 \mu\text{M}$ ) further reduced the rate of sEPSCs (by  $28.41 \pm 7.22\%$  of control in IRTX,  $n = 12$ ,  $p < 0.02$ , Figure 1e) but did not change their amplitude (by  $1.12 \pm 3.19\%$ ,  $n = 12$ ,  $p = 0.67$ ). Thus, the cannabinoid-mediated effects by NADA ( $1 \mu\text{M}$ ) are masked by its effects on TRPV1.

These results indicate that NADA activates TRPV1, but at higher concentrations ( $3$ – $10 \mu\text{M}$ ) this effect is masked by NADA activation of CB1-R. However, NADA ( $1 \mu\text{M}$ ) is able to activate CB1-R as well, when the vanilloid receptors are blocked.

Similarly, higher doses of NADA ( $10 \mu\text{M}$ ) in the presence of IRTX, significantly reduced the frequency of sEPSCs by  $58.68 \pm 11.20\%$  ( $n = 6$ ,  $p < 0.02$ ; Figure 1c and e) without affecting their amplitude ( $6.13 \pm 6.01\%$ ,  $p = 0.49$ ). Likewise, the synthetic CB1 agonist WIN55, 212-2 (WIN,  $1 \mu\text{M}$ , the dose attaining maximal effect) caused a significant reduction of sEPSC frequency ( $38.42 \pm 8.85\%$ , from  $6.76 \pm 2.07$  to  $4.04 \pm 1.24 \text{ Hz}$ ,  $n = 9$ ,  $p < 0.02$ ), but it did not change

the sEPSC amplitude ( $14.18 \pm 0.60 \text{ pA}$  in control and  $13.81 \pm 0.63 \text{ pA}$  during WIN perfusion,  $n = 9$ ,  $p = 0.32$ ). This indicates that when TRPV1 channels are blocked by IRTX, NADA ( $10 \mu\text{M}$ ) reduces glutamatergic neurotransmission to the same extent of WIN (Figure 2b, ( $2 = 0.62$ ,  $p = 0.834$ ).

Excitatory and inhibitory effects of NADA were due to the activation of TRPV1 and CB1 receptors, respectively, because in the presence of both IRTX and AM281, NADA neither modified the frequency nor the amplitude of sEPSCs ( $5.28 \pm 6.09$  and  $1.12 \pm 7.44\%$ ,  $p = 0.51$  and  $0.29$ , respectively,  $n = 6$ ; Figure 1d and e).

### NADA Disinhibits Dopamine Neurons by Activating CB1

In a previous study (Marinelli *et al*, 2003), we have demonstrated that TRPV1 activation does not modulate the GABAergic transmission on DA neurons of the substantia nigra. In contrast, stimulation of CB1-R reduces both GABA and glutamate release (Szabo *et al*, 2002a; Wallmichrath and Szabo, 2002a, b; Melis *et al*, 2004) onto these cells.

In the following experiments, we investigated the effects of NADA on spontaneous GABAergic postsynaptic currents. NADA ( $10 \mu\text{M}$ ) significantly reduced the sIPSC frequency by  $32.06 \pm 11\%$  (before drug,  $4.76 \pm 1 \text{ Hz}$ ; after drug  $3.48 \pm 0.9 \text{ Hz}$ ,  $n = 6$ ,  $p < 0.05$ ; Figure 2a and b) without changing the sIPSC amplitude (control  $20.03 \pm 3.8 \text{ pA}$ ; during drug  $19.2 \pm 5.7 \text{ pA}$ ,  $n = 6$ ,  $p = 0.16$ ). Similar data were obtained

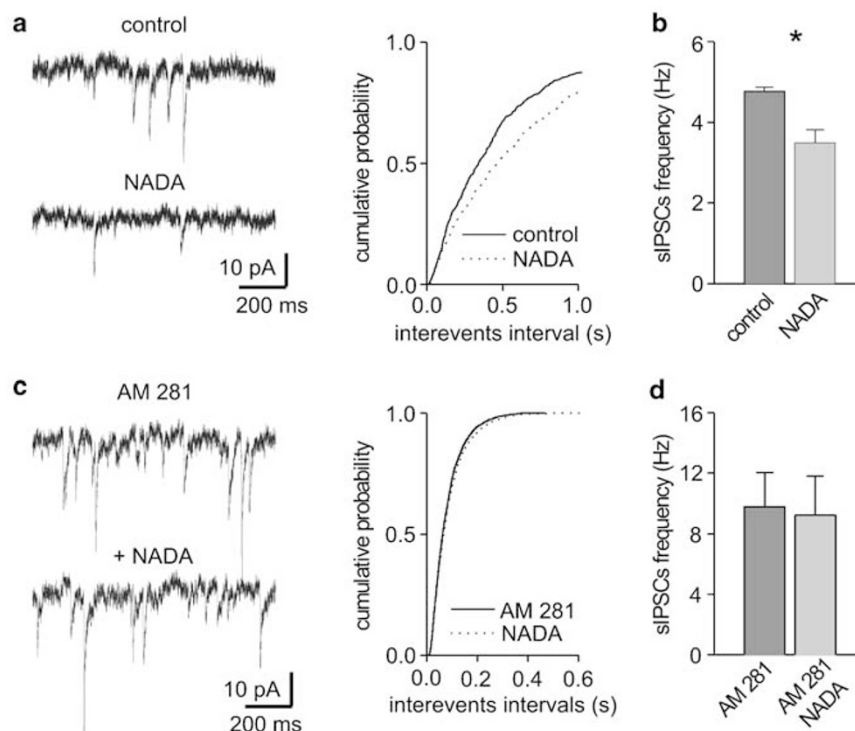


**Figure 2** NADA decreases the frequency of sIPSCs via CB1 activation. All experiments are performed in the presence of CNQX ( $10 \mu\text{M}$ ) and AP5 ( $50 \mu\text{M}$ ). (a) Top and bottom panels show trace records obtained from a DA neuron before and during  $10 \mu\text{M}$  NADA application. On the right, the cumulative curves of interevent intervals of the same neuron on the left in control (solid line) and in the presence of NADA (dotted line) are significantly different ( $p < 0.01$ , KS test). NADA shifts the cumulative distribution curve towards the right. (b) Summary of the effect of NADA on sIPSCs frequency ( $n = 6$ ,  $*p < 0.05$ , Student's *t*-test paired). (c) In the presence of AM281 ( $500 \text{ nM}$ ), NADA ( $10 \mu\text{M}$ ) did not modify the frequency of sIPSCs as shown by the trace records and cumulative curve distribution ( $p = 0.82$ , KS test). (d) Summary of NADA effects on GABAergic transmission in the presence of AM281 ( $p = 0.57$ ,  $n = 5$ , Student's *t*-test paired).

using the synthetic CB1-R agonist WIN (1  $\mu$ M), which reduced sIPSC rate by  $34.56 \pm 5.36\%$  ( $n = 7$ ,  $p < 0.05$ ) but did not significantly affect their mean amplitude ( $13.77 \pm 6.01\%$ ;  $n = 7$ ,  $p = 0.09$ ; data not shown).

In the presence of the CB1-R antagonist AM 281 (500 nM), NADA neither modified the rate nor the amplitude of sIPSCs (from  $9.79 \pm 2.26$  to  $9.23 \pm 2.58$  Hz,  $n = 5$ ,  $p = 0.54$  and from  $29.32 \pm 3.26$  to  $27.90 \pm 3.21$  pA,  $n = 5$ ,  $p = 0.095$ , respectively; Figure 2c and d). These data demonstrate that NADA, similarly to WIN ( $\chi^2 = 0.07$ ,  $p = 0.79$ ), disinhibits DA neurons via CB1 stimulation.

### Blockade of EMT Causes a Switch to the CB1-Mediated Effect of NADA

In the next set of experiments, we investigated whether NADA is taken up by cells via the putative endocannabinoid transporter, EMT (Hillard and Jarrahian, 2003), and whether EMT controls the neuromodulatory actions of NADA via TRPV1 or CB1-R. Agents able to block the EMT have been shown to facilitate endocannabinoids action at CB1 and to reduce their TRPV1-mediated effects (De Petrocellis *et al*, 2001); thus, we used a novel and selective inhibitor of endocannabinoid cellular uptake, OMDM-1 (Ortar *et al*, 2003).

Bath application of OMDM-1 (1  $\mu$ M) diminished on its own the frequency of sEPSCs from  $7.53 \pm 1.9$  to  $5.16 \pm 0.9$  Hz ( $n = 6$ ,  $p < 0.05$ ; Figure 3a) without altering sEPSC amplitude ( $13.56 \pm 1.93$  pA in control,  $12.6 \pm 2.02$ ,  $n = 6$ ,  $p = 0.09$ ). Subsequent coapplication of NADA (1  $\mu$ M) further reduced the rate of sEPSCs to  $3.06 \pm 0.74$  Hz ( $n = 6$ ,  $p < 0.02$ ; Figure 3a and b) without changing the sEPSC amplitude (to  $11.29 \pm 1.3$  pA,  $n = 6$ ,  $p = 0.1$ ). As shown in Figure 3b, the CB1-R antagonist AM281 partially counteracted the inhibitory effects of NADA on sEPSCs frequency (from  $3.06 \pm 0.74$  to  $4.26 \pm 0.33$  Hz,  $n = 6$ ,  $p = 0.52$ ). These results indicate that exogenous NADA is transported inside the cells by EMT and pharmacological blockade of this process prevents TRPV1 activation, allowing for NADA to exert uniquely a CB1-R-mediated inhibitory effect.

To test whether the above effects could be ascribed to endogenous agonists as well, we recorded sEPSCs in the presence of OMDM-1 while blocking TRPV1 with IRTX. In these conditions, the EMT blocker did not significantly decrease both sEPSC rates (from  $4.12 \pm 0.93$  to  $3.52 \pm 0.6$  Hz,  $n = 5$ ,  $p = 0.2$  Figure 3c and d) and amplitudes (from  $11.09 \pm 0.62$  to  $9.53 \pm 0.37$  pA,  $n = 5$ ,  $p = 0.18$ ).

In contrast to the effects on TRPV1, CB1-R-mediated responses were not dependent on EMT activity. This was suggested by experiments on sIPSCs, which are known to be insensitive to TRPV1 stimulation in substantia nigra (Marinelli *et al*, 2003). In the presence of CNQX, bath perfusion of OMDM-1 (1  $\mu$ M), did not significantly affect both sIPSC frequency (from  $7.83 \pm 1.41$  to  $8.01 \pm 1.5$  Hz;  $n = 4$ ,  $p = 0.56$ , not shown) and amplitude (from  $23.67 \pm 3.47$  to  $20.01 \pm 1.92$  pA,  $n = 4$ ,  $p = 0.19$ ).

### Transport of [<sup>3</sup>H]NADA by SN Slices

In order to give biochemical background to the patch-clamp recordings, we sought to measure the ability of SN slices to take up [<sup>3</sup>H]NADA. In keeping with the electrophysiological

data, we found that SN slices transported 25  $\mu$ M [<sup>3</sup>H]NADA at a rate of  $25.2 \pm 3.0$  pmol/min/mg protein at 37°C, compared to a negligible rate of  $4.0 \pm 1.0$  pmol/min per mg protein at 4°C ( $p < 0.01$  vs 37°C;  $n = 3$ ). In addition, the uptake of 25  $\mu$ M [<sup>3</sup>H]NADA at 37°C was minimized by 1  $\mu$ M OMDM-1, that reduced it down to  $7.1 \pm 1.0$  pmol/min/mg protein ( $p < 0.01$  vs control;  $n = 3$ ). Taken together, these data suggest that SN slices transported [<sup>3</sup>H]NADA through a carrier, and that the NADA transporter was at least similar to the EMT.

### Double Immunofluorescence

Confocal microscopy showed that TRPV1 immunoreactivity was present in cell bodies, dendrites, and terminals as well diffusely in the neurophil (Figure 4a–f). In the cell bodies, TRPV1 was present in both the nuclear and cytoplasmic compartments leaving the nucleoli unstained. Preliminary immunofluorescence experiments performed on juvenile rats used for electrophysiological recordings showed the same results of the adult rats. Double immunofluorescence for TRPV1 and TH showed that many TH-positive neurons presented TRPV1 immunoreactivity and that some TRPV1-positive cells were TH negative. (Figure 4a–c). No quantification was attempted. TRPV1-positive TH-negative cell bodies were scattered and some of them presented the morphological appearance of astrocytes. As TRPV1-positive astrocytes have been found in other brain areas, a double labeling between TRPV1 and an astrocyte marker was performed. This hypothesis was confirmed by TRPV1 and GFAP double immunofluorescence that showed colocalization of GFAP and TRPV1 immunoreactivities (Figure 4d–f). TRPV1 immunoreactivity was found in astrocytic cell bodies as well in processes throughout the tissue. Only some astrocytes were TRPV1 positive, indicating the presence of a subpopulation of TRPV1-expressing astrocytes. CB1-R immunofluorescence was found in cell processes, small diameter fibers, and puncta. No clear cell labeling was observed. Often CB1-R-positive processes and puncta were in close apposition with cellular profiles (Figure 4g–l). Double immunofluorescence for CB1-R and TRPV1 showed that many of CB1-R-positive processes and puncta were also TRPV1 positive. These double-labeled structures tended to surround neuronal bodies appearing either TRPV1 positive or negative (Figure 4g–l).

### DISCUSSION

The results of the present study show a complex pattern of effects mediated by NADA on DA neurons in the SNpc, via activation of TRPV1 and CB1-R. In particular, our anatomical and physiological data indicate the presence of both receptors on the same presynaptic structures and suggest the presence of CB1-R on glutamatergic and GABAergic terminals, while TRPV1 are localized on glutamatergic terminals only.

Confocal analyses demonstrate a colocalization of CB1-R and TRPV1 in punctate structures, possibly synaptic structures, in close contact with SNpc DA neurons. However, these analyses do not allow a definite characterization of the labeled structures as presynaptic elements. Nevertheless,

patch-clamp results indicating functional interactions between TRPV1 and CB1-R, particularly on putative glutamatergic terminals, strongly support the anatomical colocalization data. Moreover, previous studies sustain this suggestion indicating that excitatory afferents to SNpc origi-

nating from cortex, subthalamic nucleus, and amygdaloid complex, express mRNA for both TRPV1 and CB1-R (Mailleux and Vanderhaeghen, 1992; Matsuda et al, 1993; Mezey et al, 2000; Moldrich and Wenger, 2000; Romero et al, 2002).

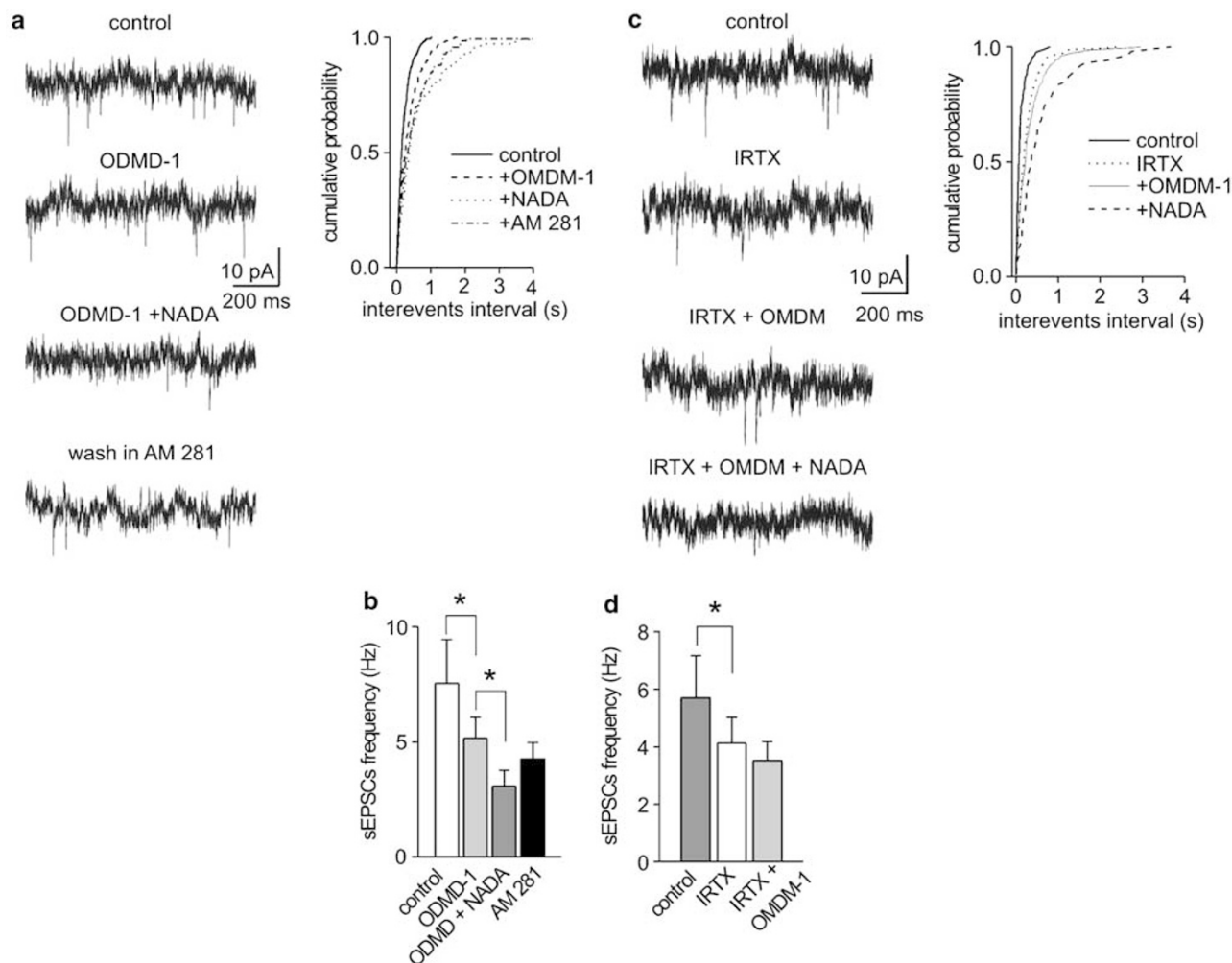
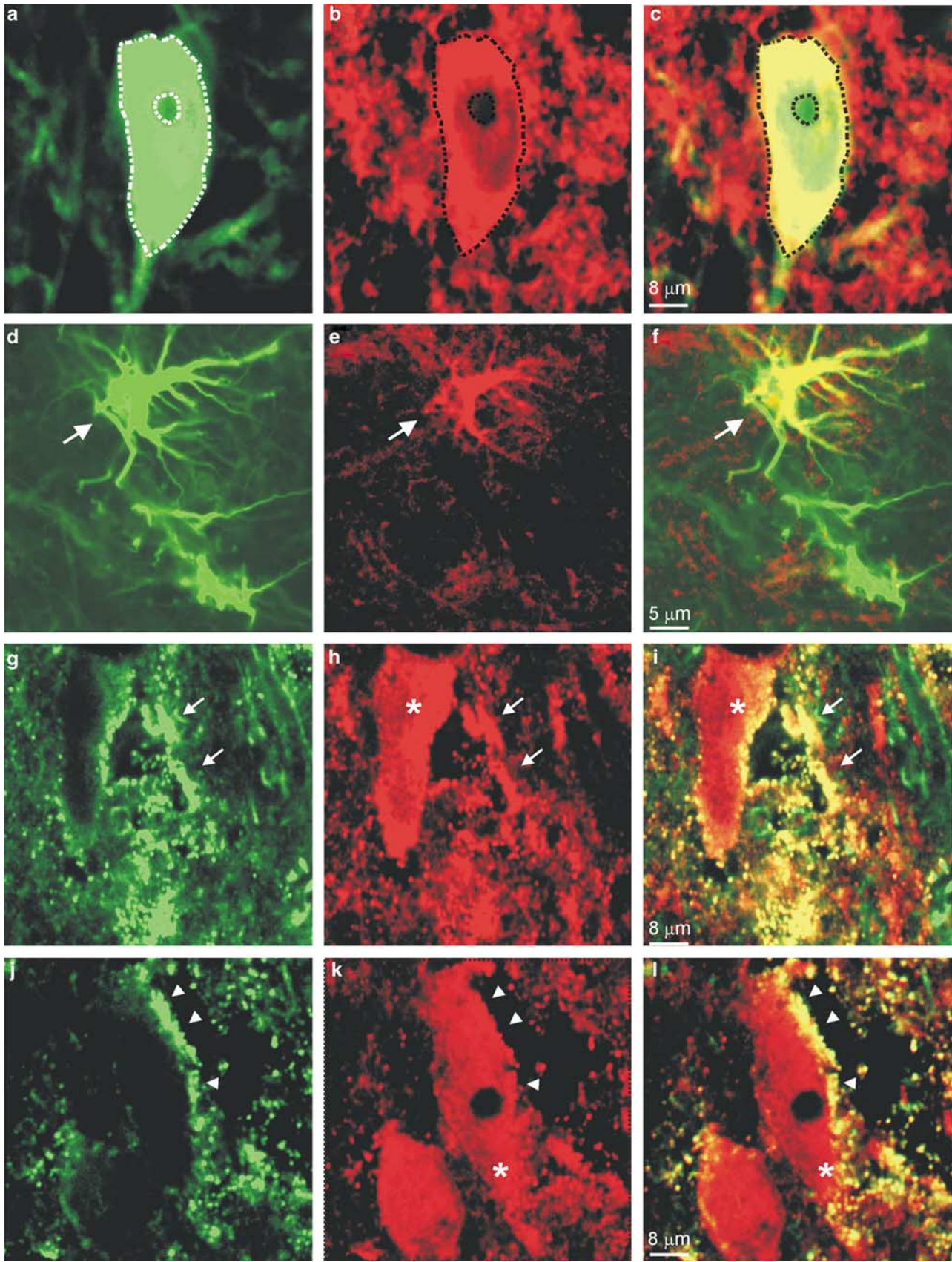


**Figure 3** NADA exerts a CB1-mediated effect when the EMT is blocked. (a) Trace records obtained from a DA neuron in control, with OMDM-1 (1  $\mu$ M), NADA (1  $\mu$ M), and after washout with the CB1-R antagonist, AM281 (500 nM). On the right, cumulative curve distributions of the same neuron on the left, in control (solid line), OMDM-1 (dashed line), during NADA superfusion (dotted line), and during washout with AM 281 (dashed dotted line). Note that OMDM-1 reduced *per se* the frequency of sEPSCs ( $p < 0.01$  KS-test). NADA further shifted the distribution curve towards the right ( $p < 0.01$  KS test). (b) Summary histogram of NADA on sEPSCs in the presence of OMDM-1. Both OMDM-1 and NADA (in OMDM-1) significantly reduced the frequency of sEPSCs (mean  $\pm$  SEM,  $n = 6$ ,  $*p < 0.05$  and  $p < 0.02$ , respectively, Student's *t*-test paired). AM 281 partially reversed the reduction caused by NADA when the EMT was blocked. (c) Sample of traces from a DA neuron in control, with IRTX (300 nM), with IRTX + OMDM-1 (1  $\mu$ M), with IRTX + OMDM-1, and NADA (10  $\mu$ M). On the right, the cumulative probability of interevent intervals from the same neuron on the left. IRTX significantly reduced the frequency of sEPSCs (KS-test  $p < 0.002$ ) while bath coapplication with OMDM-1 did not (KS-test  $p = 0.30$ ). Conversely, NADA still reduced sEPSCs frequency (KS-test  $p < 0.002$ ). All these compounds did not affect sEPSCs amplitude. (d) Summary histogram of the effect of OMDM-1 on sEPSCs in the presence of IRTX. IRTX significantly reduced the frequency of sEPSCs (mean  $\pm$  SEM,  $n = 5$ ,  $*p < 0.05$ , Student's *t*-test paired) whereas OMDM-1 did not further reduce significantly the rate of sEPSCs when coapplied with IRTX (mean  $\pm$  SEM,  $n = 5$ ,  $*p = 0.2$ , Student's *t*-test paired).

**Figure 4** Laser confocal images of double immunofluorescence for TRPV1 and TH (a–c), for TRPV1 and GFAP (d–f), and for TRPV1 and CB1 (g–i) in the substantia nigra pars compacta (SNpc). (a–c) Dopaminergic neuron positive for TRPV1. (a) TH immunoreactivity (green), (b) TRPV1 immunoreactivity (red), (c) merge. Note TRPV1 positive structures in close apposition with the neuronal membrane (outline). (d–f) Astrocyte positive for TRPV1. (d) GFAP immunoreactivity (green), (e) TRPV1 immunoreactivity (red), (f) merge. (g–i) Processes (arrow heads) and puncta (arrows) expressing both TRPV1 and CB1 in contact with TRPV1-positive neuronal cell bodies (asterisks). (g and j) CB1 immunoreactivity (green), (h and k) TRPV1 immunoreactivity (red), (i and l) merge.







Confocal microscopy analyses also suggest that CB1-R expression is only presynaptic, whereas TRPV1 can be both pre- and postsynaptic as previously reported in rat spinal cord (Valtschanoff *et al*, 2001). The functional role of postsynaptic TRPV1 still needs to be identified, as our electrophysiological observations only refer to the presynaptic function of this receptor (see below). TRPV1 immunoreactivity is present in dopaminergic cell bodies and dendrites as well as in astrocytes. The presence of TRPV1 in the neuronal bodies and dendrites has been already shown in different areas of the brain (Mezey *et al*, 2000; Toth *et al*, 2005). So far, the TRPV1 expression has been demonstrated in astrocytes and pericytes in different areas of the CNS (Doyle *et al*, 2002; Toth *et al*, 2005). Interestingly, the localization of TRPV1 on both neurons and glia suggest the hypothesis of a functional neuron–glia crosstalk sustained through this receptor. The functional role of TRPV1 expression in glial cells is intriguing and will be addressed in future experiments.

NADA is an endogenous molecule present in several brain areas (Huang *et al*, 2002b). In control midbrain slices, we could not detect significant levels of NADA, probably because it was below the detection limit of the assay (<0.5 pmol). Indeed, after stimulation by high potassium, a component with the characteristics of NADA (retention time and molecular mass) was detected. This could be explained by the fact that NADA is mainly synthesized in areas not included within our slice preparation, so that only terminals from those areas can release this mediator following depolarization with high potassium. A possible candidate could be the striatum, which has been shown to contain high levels of NADA (Huang *et al*, 2002b). Preliminary data indicate that, indeed, NADA is produced in the striatum from the condensation of DA and arachidonic acid, and not from the transformation of *N*-arachidonoyl-tyrosine (Michael J Walker, personal communication and V Di Marzo, unpublished observations). However, the enzyme catalyzing the formation of NADA has not been identified yet, nor it is known if, as possibly suggested by the present data, it is a Ca<sup>2+</sup>-sensitive protein as in the case of AEA-biosynthesizing enzymes.

By using patch-clamp recordings, we found that exogenously applied NADA (10 μM)-enhanced or reduced glutamatergic neurotransmission by a presynaptic mechanism, when coapplied with the CB1-R or TRPV1 antagonist, AM281 and IRTX, respectively. Remarkably, exogenously applied NADA could facilitate glutamate release via TRPV1 even in the absence of the CB1-R antagonist, when tested at low doses (1 μM). This is in agreement with a reported higher effect of NADA at TRPV1 than at CB1-R (Bisogno *et al*, 2000; Huang *et al*, 2002b). It is worth to note that NADA, when applied at a high dose (10 μM) and in the absence of either CB1-R or TRPV1 antagonists, did not significantly modify glutamate transmission to the DA neurons. The lack of effects might be due to the simultaneous activation of CB1-R and TRPV1, giving rise to opposing actions. When compared to our previous experiments (Marinelli *et al*, 2003), and in line with other *in vitro* studies (Huang *et al*, 2002b; Harrison *et al*, 2003; Price *et al*, 2004), the TRPV1-mediated increase of glutamatergic transmission by NADA or by the exogenous TRPV1 agonist capsaicin, was significantly higher than that induced by AEA. In fact, AEA did not produce any significant facili-

tation of glutamate release unless coapplied with the adenylate cyclase activator forskolin (Marinelli *et al*, 2003).

The presynaptic distribution of CB1-R in the SNpc here reported is in line with the presynaptic effects on glutamate and GABA release by NADA and its synthetic cannabinoid agonist WIN. This is in agreement with earlier studies reporting a presynaptic modulation of neurotransmission by CB1-R in several brain regions, especially in the ventral midbrain (Szabo *et al*, 2000; Gerdeman and Lovinger, 2001; Huang *et al*, 2001, 2002a; Azad *et al*, 2003; Melis *et al*, 2004).

Similarly to what has been previously observed for AEA (De Petrocellis *et al*, 2001), the vanilloid and cannabinoid effects of NADA shown in this study appear to depend on the cellular distribution of CB1-R and TRPV1 binding sites in the extracellular and intracellular milieu, respectively. The binding site for capsaicin and AEA on TRPV1 has been found in a cytosolic domain of this channel (Jordt and Julius, 2002); therefore, these compounds must cross the plasma membrane in order to stimulate TRPV1 (De Petrocellis *et al*, 2001). With regard to NADA, this compound is rapidly taken up by C6 glioma cells via a facilitated diffusion process similar to that of AEA (Huang *et al*, 2002b). We now show that, when this transport process is blocked by the selective EMT inhibitor OMDM-1, the effects of NADA at TRPV1 are abolished, whereas those through CB1-R are favored. Thus, it appears that NADA, like AEA, must be taken up by cells in order to interact with the intracellular binding site of TRPV1. Such phenomenon has recently been reported also for TRPV1-mediated actions by NADA and AEA in trigeminal neurons (Price *et al*, 2005). Although the exact binding site of NADA on TRPV1 has not been identified yet, its chemical similarity with AEA might suggest that NADA uses the same intracellular domain implicated in AEA binding to this channel. Unfortunately, to date, there is no molecular evidence for the expression of EMT. However, selective endocannabinoid uptake inhibitors, such as OMDM-1, are useful pharmacological tools to study its functional role. Even though such tools do not allow to establish the exact localization of this putative protein at the pre- or post-synaptic level, functional evidence suggests the existence of a postsynaptic transporter mechanism in striatal neurons (Ronesi *et al*, 2004).

Interestingly, we have shown that OMDM-1 reduced *per se* the frequency of sEPSCs, whereas it did not affect GABAergic synapses, as they are not under the control of TRPV1 (Marinelli *et al*, 2003). Inhibition of glutamatergic transmission by NADA in the presence of OMDM-1 was not completely reverted by the CB1-R antagonist AM 281 (Figure 3b), indicating that this effect was not due just to an increased action onto CB1-R by endogenous compounds, but also to inhibition of a tonic facilitatory control through TRPV1. This hypothesis is confirmed by the lack of the effects of OMDM-1 on the glutamatergic transmission when the TRPV1 are blocked and supported by our previous finding of a tonic facilitation of glutamate release by TRPV1 (Marinelli *et al*, 2003). Thus, these results may be seen as further evidence that, at least in our experimental conditions, the excitatory inputs onto DA neurons are under TRPV1 tonic control. With regard to CB1-R, they have been shown to exert a tonic inhibition at GABAergic terminal onto the DA neurons (Yanovsky *et al*, 2003), while at

glutamatergic synapses their effect becomes evident only upon DA neurons depolarization (Melis *et al*, 2004).

In conclusion, NADA can exert opposing actions on DA neurons via activation of TRPV1 or CB1-R: an excitatory effect, exerted by increasing glutamatergic (through TRPV1) and decreasing GABAergic transmission (through CB1-R), and an inhibitory one, occurring through a decrease of glutamatergic transmission (through CB1-R only).

It might be speculated that activation of either TRPV1 or CB1-R through NADA may be dependent on the functional state of the dopamine system. As NADA levels strongly depend on those of dopamine (JM Walker, personal communication to VDM), it is possible that, whereas low levels of NADA preferentially activate the vanilloid receptors with subsequent glutamate release, a progressive increase in neuronal excitation is expected to lead to higher levels of this compound, and thus to retrograde activation of CB1-R and of its subsequent inhibitory effects on glutamatergic signaling.

## ACKNOWLEDGEMENTS

We thank Dr N Berretta, for the helpful discussion and for reading the manuscript.

## REFERENCES

- Ahluwalia J, Urban L, Bevan S, Capogna M, Nagy I (2002). Cannabinoid 1 receptors are expressed by nerve growth factor- and glial cell-derived neurotrophic factor-responsive primary sensory neurons. *Neuroscience* **110**: 747–753.
- Ahluwalia J, Urban L, Capogna M, Bevan S, Nagy I (2000). Cannabinoid 1 receptors are expressed in nociceptive primary sensory neurons. *Neuroscience* **100**: 685–688.
- Al-Hayani A, Wease KN, Ross RA, Pertwee RG, Davies SN (2001). The endogenous cannabinoid anandamide activates vanilloid receptors in the rat hippocampal slice. *Neuropharmacology* **41**: 1000–1005.
- Azad SC, Eder M, Marsicano G, Lutz B, Zieglansberger W, Rammes G (2003). Activation of the cannabinoid receptor type 1 decreases glutamatergic and GABAergic synaptic transmission in the lateral amygdala of the mouse. *Learn Mem* **10**: 116–128.
- Beltramo M, Stella N, Calignano A, Lin SY, Makriyannis A, Piomelli D (1997). Functional role of high-affinity anandamide transport, as revealed by selective inhibition. *Science* **277**: 1094–1097.
- Bezuglov V, Bobrov M, Gretskeya N, Gonchar A, Zinchenko G, Melck D *et al* (2001). Synthesis and biological evaluation of novel amides of polyunsaturated fatty acids with dopamine. *Bioorg Med Chem Lett* **11**: 447–449.
- Bisogno T, Melck D, Bobrov M, Gretskeya NM, Bezuglov VV, De Petrocellis L *et al* (2000). *N*-acyl-dopamines: novel synthetic CB(1) cannabinoid-receptor ligands and inhibitors of anandamide inactivation with cannabimimetic activity *in vitro* and *in vivo*. *Biochem J* **351**(Part 3): 817–824.
- Caterina MJ, Julius D (2001). The vanilloid receptor: a molecular gateway to the pain pathway. *Annu Rev Neurosci* **24**: 487–517.
- Cravatt BF, Demarest K, Patricelli MP, Bracey MH, Giang DK, Martin BR *et al* (2001). Supersensitivity to anandamide and enhanced endogenous cannabinoid signaling in mice lacking fatty acid amide hydrolase. *Proc Natl Acad Sci USA* **98**: 9371–9376.
- Cristino L, de Petrocellis L, Pryce G, Baker D, Guglielmotti V, Di Marzo V (2006). Immunohistochemical localization of cannabinoid type 1 and vanilloid transient receptor potential vanilloid type 1 receptors in the mouse brain. *Neuroscience* **139**: 1405–1415.
- De Petrocellis L, Bisogno T, Maccarrone M, Davis JB, Finazzi-Agro A, Di Marzo V (2001). The activity of anandamide at vanilloid VR1 receptors requires facilitated transport across the cell membrane and is limited by intracellular metabolism. *J Biol Chem* **276**: 12856–12863.
- Di Marzo V, Bisogno T, De Petrocellis L (2001). Anandamide: some like it hot. *Trends Pharmacol Sci* **22**: 346–349.
- Di Marzo V, Fontana A, Cadas H, Schinelli S, Cimino G, Schwartz JC *et al* (1994). Formation and inactivation of endogenous cannabinoid anandamide in central neurons. *Nature* **372**: 686–691.
- Doyle MW, Bailey TW, Jin YH, Andresen MC (2002). Vanilloid receptors presynaptically modulate cranial visceral afferent synaptic transmission in nucleus tractus solitarius. *J Neurosci* **22**: 8222–8229.
- Fegley D, Kathuria S, Mercier R, Li C, Goutopoulos A, Makriyannis A *et al* (2004). Anandamide transport is independent of fatty-acid amide hydrolase activity and is blocked by the hydrolysis-resistant inhibitor AM1172. *Proc Natl Acad Sci USA* **101**: 8756–8761.
- Fezza F, Battista N, Bari M, Maccarrone M (2006). Methods to assay anandamide hydrolysis and transport in synaptosomes. *Methods Mol Med* **123**: 163–168.
- Gerdeman G, Lovinger DM (2001). CB1 cannabinoid receptor inhibits synaptic release of glutamate in rat dorsolateral striatum. *J Neurophysiol* **85**: 468–471.
- Harrison S, De Petrocellis L, Trevisani M, Benvenuti F, Bifulco M, Geppetti P *et al* (2003). Capsaicin-like effects of *N*-arachidonoyl-dopamine in the isolated guinea pig bronchi and urinary bladder. *Eur J Pharmacol* **475**: 107–114.
- Hillard CJ, Jarrahian A (2003). Cellular accumulation of anandamide: consensus and controversy. *Br J Pharmacol* **140**: 802–808.
- Howlett AC (2002). The cannabinoid receptors. *Prostaglandins Other Lipid Mediat* **68–69**: 619–631.
- Huang CC, Chen YL, Lo SW, Hsu KS (2002a). Activation of cAMP-dependent protein kinase suppresses the presynaptic cannabinoid inhibition of glutamatergic transmission at corticostriatal synapses. *Mol Pharmacol* **61**: 578–585.
- Huang CC, Lo SW, Hsu KS (2001). Presynaptic mechanisms underlying cannabinoid inhibition of excitatory synaptic transmission in rat striatal neurons. *J Physiol* **532**: 731–748.
- Huang SM, Walker JM (2006). Enhancement of spontaneous and heat-evoked activity in spinal nociceptive neurons by the endovanilloid/endocannabinoid *N*-arachidonoyldopamine (NADA). *J Neurophysiol* **95**: 1207–1212.
- Huang SM, Bisogno T, Trevisani M, Al-Hayani A, De Petrocellis L, Fezza F *et al* (2002b). An endogenous capsaicin-like substance with high potency at recombinant and native vanilloid VR1 receptors. *Proc Natl Acad Sci USA* **99**: 8400–8405.
- Jordt SE, Julius D (2002). Molecular basis for species-specific sensitivity to ‘hot’ chili peppers. *Cell* **108**: 421–430.
- Julian MD, Martin AB, Cuellar B, Rodriguez De Fonseca F, Navarro M, Moratalla R *et al* (2003). Neuroanatomical relationship between type 1 cannabinoid receptors and dopaminergic systems in the rat basal ganglia. *Neuroscience* **119**: 309–318.
- Kim SR, Lee da Y, Chung ES, Oh UT, Kim SU, Jin BK (2005). Transient receptor potential vanilloid subtype 1 mediates cell death of mesencephalic dopaminergic neurons *in vivo* and *in vitro*. *J Neurosci* **25**: 662–671.
- Maccarrone M, Gubellini P, Bari M, Picconi B, Battista N, Centonze D *et al* (2003). Levodopa treatment reverses endocannabinoid system abnormalities in experimental parkinsonism. *J Neurochem* **85**: 1018–1025.
- Mailleux P, Vanderhaeghen JJ (1992). Distribution of neuronal cannabinoid receptor in the adult rat brain: a comparative

- receptor binding radioautography and *in situ* hybridization histochemistry. *Neuroscience* **48**: 655–668.
- Marinelli S, Di Marzo V, Berretta N, Matias I, Maccarrone M, Bernardi G *et al* (2003). Presynaptic facilitation of glutamatergic synapses to dopaminergic neurons of the rat substantia nigra by endogenous stimulation of vanilloid receptors. *J Neurosci* **23**: 3136–3144.
- Marinelli S, Pascucci T, Bernardi G, Puglisi-Allegra S, Mercuri NB (2005). Activation of TRPV1 in the VTA excites dopaminergic neurons and increases chemical- and noxious-induced dopamine release in the nucleus accumbens. *Neuropsychopharmacology* **30**: 864–870.
- Marsicano G, Wotjak CT, Azad SC, Bisogno T, Rammes G, Cascio MG *et al* (2002). The endogenous cannabinoid system controls extinction of aversive memories. *Nature* **418**: 530–534.
- Matsuda LA, Bonner TI, Lolait SJ (1993). Localization of cannabinoid receptor mRNA in rat brain. *J Comp Neurol* **327**: 535–550.
- Melis M, Pistis M, Perra S, Muntoni AL, Pillolla G, Gessa GL (2004). Endocannabinoids mediate presynaptic inhibition of glutamatergic transmission in rat ventral tegmental area dopamine neurons through activation of CB1 receptors. *J Neurosci* **24**: 53–62.
- Mercuri NB, Bonci A, Calabresi P, Bernardi G (1996). Characterization of a barium-sensitive outward current following glutamate application on rat midbrain dopaminergic cells. *Eur J Neurosci* **8**: 1780–1786.
- Mezey E, Toth ZE, Cortright DN, Arzubi MK, Krause JE, Elde R *et al* (2000). Distribution of mRNA for vanilloid receptor subtype 1 (VR1), and VR1-like immunoreactivity, in the central nervous system of the rat and human. *Proc Natl Acad Sci USA* **97**: 3655–3660.
- Moldrich G, Wenger T (2000). Localization of the CB1 cannabinoid receptor in the rat brain. An immunohistochemical study. *Peptides* **21**: 1735–1742.
- Ortar G, Ligresti A, De Petrocellis L, Morera E, Di Marzo V (2003). Novel selective and metabolically stable inhibitors of anandamide cellular uptake. *Biochem Pharmacol* **65**: 1473–1481.
- O'Sullivan SE, Kendall DA, Randall MD (2004). Characterisation of the vasorelaxant properties of the novel endocannabinoid *N*-arachidonoyl-dopamine (NADA). *Br J Pharmacol* **141**: 803–812.
- Pazos MR, Nunez E, Benito C, Tolon RM, Romero J (2005). Functional neuroanatomy of the endocannabinoid system. *Pharmacol Biochem Behav* **81**: 239–247.
- Pettit DA, Harrison MP, Olson JM, Spencer RF, Cabral GA (1998). Immunohistochemical localization of the neural cannabinoid receptor in rat brain. *J Neurosci Res* **51**: 391–402.
- Price TJ, Patwardhan A, Akopian AN, Hargreaves KM, Flores CM (2004). Modulation of trigeminal sensory neuron activity by the dual cannabinoid–vanilloid agonists anandamide, *N*-arachidonoyl-dopamine and arachidonoyl-2-chloroethylamide. *Br J Pharmacol* **141**: 1118–1130.
- Price TJ, Patwardhan AM, Flores CM, Hargreaves KM (2005). A role for the anandamide membrane transporter in TRPV1-mediated neurosecretion from trigeminal sensory neurons. *Neuropharmacology* **49**: 25–39.
- Romero J, Lastres-Becker I, de Miguel R, Berrendero F, Ramos JA, Fernandez-Ruiz J (2002). The endogenous cannabinoid system and the basal ganglia. Biochemical, pharmacological, and therapeutic aspects. *Pharmacol Ther* **95**: 137–152.
- Ronesi J, Gerdeman GL, Lovinger DM (2004). Disruption of endocannabinoid release and striatal long-term depression by postsynaptic blockade of endocannabinoid membrane transport. *J Neurosci* **24**: 1673–1679.
- Sagar DR, Smith PA, Millns PJ, Smart D, Kendall DA, Chapman V (2004). TRPV1 and CB(1) receptor-mediated effects of the endovanilloid/endocannabinoid *N*-arachidonoyl-dopamine on primary afferent fibre and spinal cord neuronal responses in the rat. *Eur J Neurosci* **20**: 175–184.
- Szabo B, Siemes S, Wallmichrath I (2002a). Inhibition of GABAergic neurotransmission in the ventral tegmental area by cannabinoids. *Eur J Neurosci* **15**: 2057–2061.
- Szabo B, Wallmichrath I, Mathonia P, Pfreundtner C (2000). Cannabinoids inhibit excitatory neurotransmission in the substantia nigra pars reticulata. *Neuroscience* **97**: 89–97.
- Szabo T, Biro T, Gonzalez AF, Palkovits M, Blumberg PM (2002b). Pharmacological characterization of vanilloid receptor located in the brain. *Brain Res Mol Brain Res* **98**: 51–57.
- Toth A, Boczan J, Kedei N, Lizanecz E, Bagi Z, Papp Z *et al* (2005). Expression and distribution of vanilloid receptor 1 (TRPV1) in the adult rat brain. *Brain Res Mol Brain Res* **135**: 162–168.
- Tsou K, Brown S, Sanudo-Pena MC, Mackie K, Walker JM (1998). Immunohistochemical distribution of cannabinoid CB1 receptors in the rat central nervous system. *Neuroscience* **83**: 393–411.
- Valtschanoff JG, Rustioni A, Guo A, Hwang SJ (2001). Vanilloid receptor VR1 is both presynaptic and postsynaptic in the superficial laminae of the rat dorsal horn. *J Comp Neurol* **436**: 225–235.
- Wallmichrath I, Szabo B (2002a). Cannabinoids inhibit striatonigral GABAergic neurotransmission in the mouse. *Neuroscience* **113**: 671–682.
- Wallmichrath I, Szabo B (2002b). Analysis of the effect of cannabinoids on GABAergic neurotransmission in the substantia nigra pars reticulata. *Naunyn Schmiedeberg's Arch Pharmacol* **365**: 326–334.
- Yanovsky Y, Mades S, Misgeld U (2003). Retrograde signaling changes the venue of postsynaptic inhibition in rat substantia nigra. *Neuroscience* **122**: 317–328.